

# The lithospheric structure along profile Vyhne based on 2D integrated geophysical modelling (Western Carpathians, Slovakia)

Jana DÉREROVÁ<sup>1,\*</sup> , Miroslav BIELIK<sup>1,2</sup> , Irina MAKARENKO<sup>3</sup> ,  
Olga LEGOSTAEVA<sup>3</sup> , Igor KOHÚT<sup>1</sup> , Jozef BÓDI<sup>1,2,4</sup> 

<sup>1</sup> Division of Geophysics, Earth Science Institute of the Slovak Academy of Sciences,  
Dúbravská cesta 9, 841 04 Bratislava, Slovak Republic

<sup>2</sup> Department of Engineering Geology, Hydrogeology and Applied Geophysics,  
Faculty of Natural Sciences, Comenius University in Bratislava,  
Mlynská dolina, Ilkovičova 6, Bratislava, 842 15, Slovak Republic

<sup>3</sup> S. Subbotin Institute of Geophysics of the National Academy of Sciences of Ukraine,  
32, Akademika Palladina avenue, Kyiv, 03680, Ukraine

<sup>4</sup> Institute of Geosciences (CSIC-UCM),  
C/Doctor Severo Ochoa, 7, 28040, Madrid, Spain

**Abstract:** We have used 2D integrated modelling method to derive a model of the lithospheric structure along profile Vyhne located in the Western Carpathians. The algorithm determines the thermal structure of the lithosphere that is controlled by other geophysical fields, namely by heat flow, topography, gravity and geoid data. Such approach allows us to distinguish between density variations at different depths. Integrated algorithm method focuses primarily on the analysis of deeper lithospheric structure, especially on the lithosphere–asthenosphere boundary (LAB). Beneath the European Platform and the Outer Western Carpathians, the LAB is nearly horizontal, lying at depths of approximately 115–118 km. Moving toward the Inner Western Carpathians, a modest increase in lithospheric thickness becomes apparent, along with the presence of a subtly developed lithospheric root, which may represent a small remnant of the upper part of the break-off subducted lithospheric slab. Based on the computed thermal structure of the lithosphere, we established a rheological model along this profile. We determined the lithospheric strength distribution (considering both brittle and ductile deformation) for compressional and extensional settings, calculated the vertically integrated strength, and constructed the yield-strength envelope for the tectonic environment of the Vyhne tidal station. Our findings clearly indicate that a compressional regime prevails, with the greatest strength beneath the European Platform and the Western Carpathians. Along the modelled profile, strength declines from the high values observed beneath the European Platform to a

\*corresponding author: e-mail: Jana.Dererova@savba.sk

minimum within the Pieniny Klippen Belt before rising again to peak values beneath the Western Carpathians.

**Key words:** integrated geophysical modelling, heat flow, topography, gravity, geoid, lithosphere, asthenosphere, rheology, strength, Vyhne, tidal station, Western Carpathians

## 1. Introduction

The Western Carpathians (Fig. 1) represent the northernmost, west–east oriented orocline of the European Alpine system, lying between the Eastern Alps to the west and the Eastern Carpathians to the east (Plašienka, 2003; Froitzheim *et al.*, 2008). To the north, the Western Carpathians neighbours with the Carpathian Foredeep and the European Platform, which includes a Palaeozoic-aged basement consolidated during the Variscan orogeny and its post-Variscan sedimentary cover (Ziegler, 1990; Dadlez *et al.*, 2005). This platform incorporates the Bohemian Massif in the northwest and the Polish Platform further north (Golonka *et al.*, 2000). Toward the northeast, it is separated from the Fennosarmatian (East European) Platform by the Teisseyre–Tornquist Zone (TTZ) (Pharaoh, 1999; Mazur *et al.*, 2018).

Much of the central and inner portions of the Western Carpathians are overlain by thick Tertiary sediments and volcanic rocks, associated with the evolution of the Pannonian back-arc basin system (Royden and Horváth, 1988; Csontos and Vörös, 2004). The present-day structural architecture of the Western Carpathians developed through subduction and collisional events that took place from the Late Jurassic to the Tertiary, within the Tethyan mobile belt situated between the stable European Platform and continental fragments derived from Apulia/Adria (Plašienka *et al.*, 1997; Schmid *et al.*, 2008).

A notable aspect of the Alpine (Alpidic) evolution of the Western Carpathians is the pronounced northward progression of both pre-orogenic and orogenic stages. These include Mesozoic rifting and extension of the Variscan continental crust, subsequent crustal shortening and nappe stacking, as well as the compression and subduction of longitudinal oceanic basins (Plašienka *et al.*, 1997; Kováč, 2000). Later stages of deformation were often characterised by transpressional and transtensional tectonics that followed the main compressional phases (Kováč *et al.*, 1994; Lexa and Konečný, 1998).

The Western Carpathian orogeny waned during the Late Tertiary, following slab detachment that marked the end of southeast-directed subduction of the oceanic crust beneath the Outer Carpathian Flysch Belt (Tomek and Hall, 1993; Kováč *et al.*, 2017).

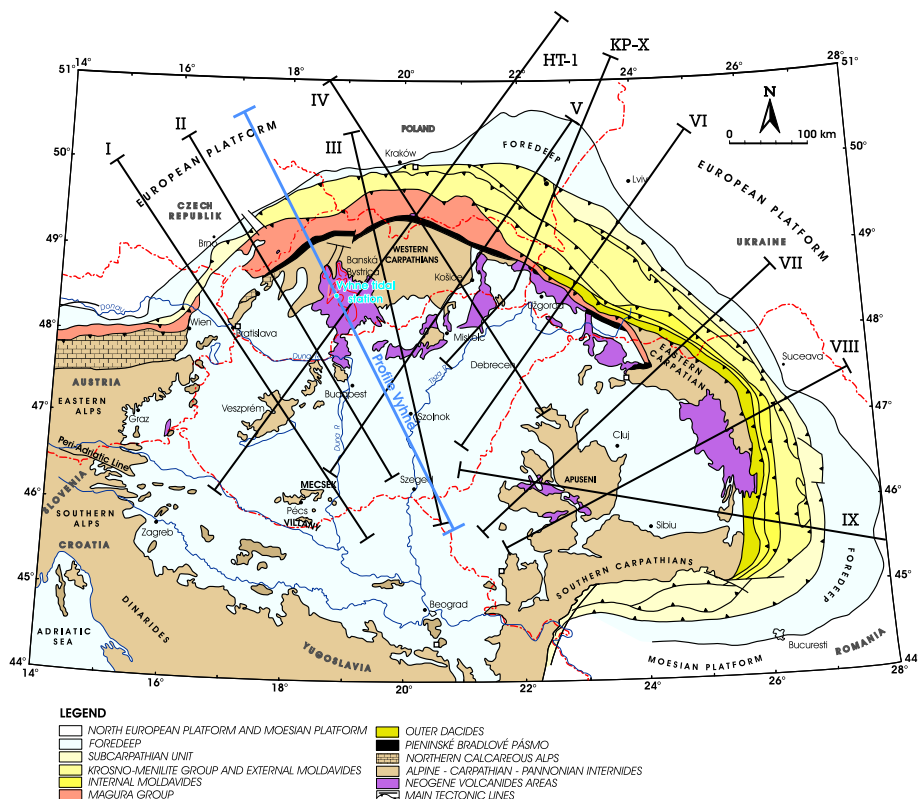


Fig. 1. Location of profile Vyhne on the map of the European platform-Carpathian-Pannonian region. The profiles I-IX were modelled in the papers of Zeyen *et al.* (2002) and Dérerová *et al.* (2006).

## 2. Profile Vyhne

The profile Vyhne starts in the Polish–European platform near Opole (50.59° N, 17.08° E), continues via the Western Carpathian molasse Foredeep, the Outer Western Carpathian flysch belt, the Pieniny Klippen Belt and the In-

ner Western Carpathians including the Tatic, Veporic, and Gemicic units, then traverses the Central Slovak Volcanic Field and adjacent Neogene extensional basins, and finally terminates in the Pannonian Basin near Szeged ( $45.82^{\circ}$  N,  $20.85^{\circ}$  E). The direction of the profile was chosen to meet the condition of perpendicularity to the studied geological units of the Carpathian orogenic system. Its total length is about 600 km, and the distribution of the main geological structures along the profile is illustrated in Fig. 1.

The Vyhne tidal station lies along the studied profile in Central Slovakia, in the central part of the Štiavnické vrchy Mountains, within the Inner Western Carpathians. It is situated in the cadaster of Vyhne village, approximately 10 km northwest of Banská Štiavnica, at an elevation of 420 m a.s.l. ( $48.50^{\circ}$  N,  $18.83^{\circ}$  E). The station is installed in the St. Anthony of Padua gallery, which provides stable underground conditions for geophysical monitoring (Brimich *et al.*, 2016).

Geologically, the area represents a complex structural zone composed of Palaeozoic crystalline rocks, Mesozoic sedimentary sequences, and Neogene volcanic and intrusive formations (Brimich, 1988; Konečný *et al.*, 2001; Lexa *et al.*, 1999). The basement consists mainly of Carboniferous granites of Variscan age, forming part of the Vyhne massif, which were affected by multiple tectonic phases (Dudášová, 1998; Brimich *et al.*, 2016). During the Late Palaeozoic, strong NW–SE-trending fault zones developed, repeatedly reactivated throughout later geological periods (Brimich, 1988; Hók *et al.*, 2000). A major NE–SW-oriented fault system established in the Mesozoic further divided the region, separating the rising Hodruša–Vyhne island block from the adjacent subsiding depression to the southeast (Brimich, 1988). Subsequent Middle Miocene granodiorite and diorite intrusions, together with the underlying Carboniferous granite, created a relatively rigid basement framework, while the marginal fault zones remained tectonically active and fractured (Konečný *et al.*, 2001; Lexa *et al.*, 1999; Lexa *et al.*, 2010). The St. Anthony gallery is predominantly excavated within Palaeozoic granite affected by two major deformation events: an early mylonitization phase and a later magmatic–hydrothermal phase, associated with the emplacement of young intrusions and mineralization (Dudášová, 1998; Lexa *et al.*, 2010). At about 43 m from the gallery entrance, a younger dacite dyke intrudes the granitic body along a north–south direction, beyond which the rocks are comparatively massive and less fractured (Brimich *et al.*, 2016).

The gallery also follows a mylonitic vein zone with quartz lenses, and locally unstable segments are reinforced by protective masonry (Dudášová, 1998). The geological configuration of the Vyhne site thus reflects the interaction of Variscan basement structures, Mesozoic fault reactivation, and Neogene magmatic activity, making it a representative locality within the Inner Western Carpathian volcanic–tectonic zone along the regional profile (Kováč *et al.*, 1994; Lexa *et al.*, 2010).

### 3. Method

The lithospheric structure along the Vyhne profile (Fig. 1) was determined using a two-dimensional (2D) integrated geophysical modelling approach, which simultaneously interprets gravity, geoid, topography, and surface heat-flow data (Dérerová *et al.*, 2006). The method, originally developed by Zeyen and Fernández (1994) and refined by Zeyen *et al.* (2005), provides a consistent framework for constraining the thermal and density structure of the lithosphere. A finite-element algorithm was applied to calculate the steady-state temperature field, with the lithospheric thickness defined by the 1300 °C isotherm. Thermal conductivity and radiogenic heat production were varied with depth, and the resulting temperature field was used to compute densities as functions of temperature and pressure, assuming a thermal expansion coefficient of  $3 \cdot 10^{-5} \text{ K}^{-1}$ . The resulting density model was applied to calculate gravity anomalies (Talwani *et al.*, 1959), topography under local isostatic equilibrium (Lachenbruch and Morgan, 1990), and geoid undulations (Zeyen *et al.*, 2005). The combined interpretation of these datasets enables discrimination between shallow crustal and deep lithospheric density variations. Gravity data primarily constrain the upper crust, while geoid and topography provide information on deeper, temperature-controlled density variations. Using the computed temperature field, the rheological structure was derived by evaluating the brittle and ductile strength components. Brittle strength follows the frictional sliding law of Byerlee (1978), while ductile strength is based on power-law creep (Lynch and Morgan, 1987; Ranalli, 1995). The resulting lithospheric strength envelope highlights the distribution of mechanically strong and weak zones, offering insight into the geodynamic evolution of the Western Carpathian lithosphere (Bielik *et al.*, 2010; Zeyen *et al.*, 2002).

## 4. Initial model

The initial layout of the lithosphere along the profile Vyhne (Fig. 2) was prepared using the following sources. The sedimentary layer in the starting

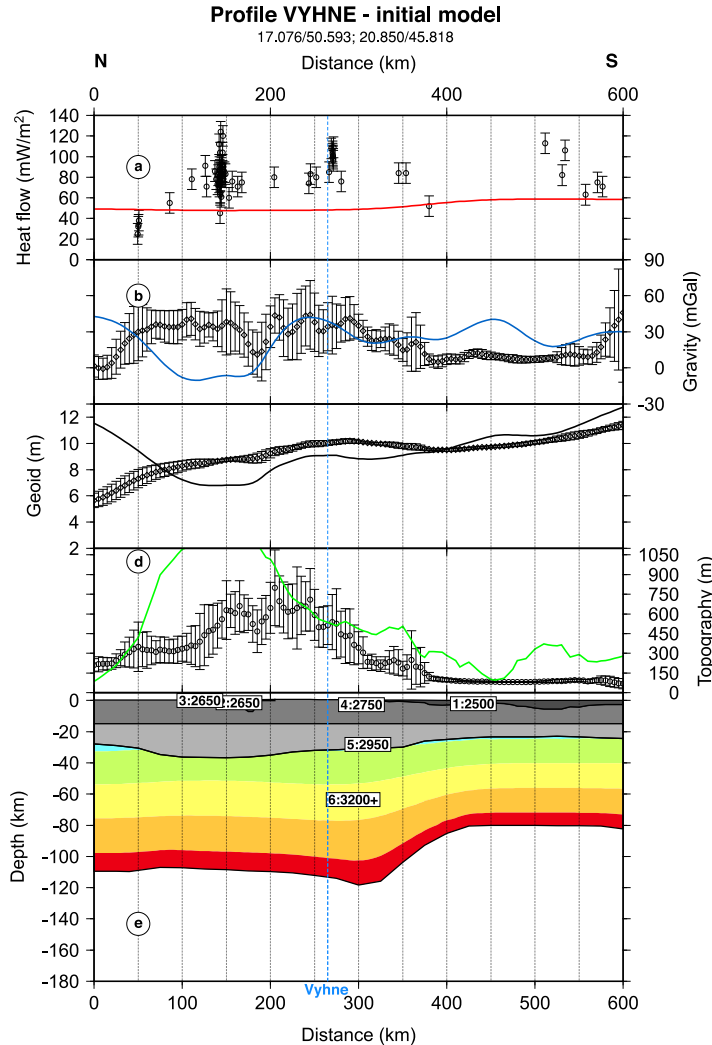


Fig. 2. Initial lithospheric model along profile Vyhne. (a) Surface heat flow, (b) free air gravity anomaly, (c) geoid, (d) topography with dots corresponding to measured data with uncertainty bars and solid lines to calculated values.

model was defined according to the data published by *Kilényi and Šefara (1989)*, *Krejčí and Jurová (1997)*, and *Makarenko et al. (2002)*. The depth of the upper–lower crust boundary was adopted from the study of *Bielik (1995)*. The Moho boundary was taken from the map presented by *Bielik et al. (2018)*. The preliminary trend of the lithosphere–asthenosphere boundary (LAB) was derived by extrapolating values from the lithospheric thickness map of *Dérerová et al. (2006)*.

The surface heat flow data were compiled from the worldwide data set of *Pollack et al. (1993)*. Topography data were taken from the GTOPO30 database (*Gesch et al., 1999*) and the free air gravity anomalies from the TOPEX 1-min gravity data set (<ftp://topex.ucsd.edu/pub> (*Sandwell and Smith, 1997*)). Geoid data were prepared based on the EGM-2008 global model (*Pavlis et al., 2008*). Geoid component corresponding to the spherical harmonics up to degree and order 8 has been removed, to avoid effects of sub-lithospheric density variations on the geoid (*Zeyen et al., 2005; Dérerová et al., 2006*). For each geophysical dataset, we have extracted several parallel profiles to calculate the lateral variability of the data.

## 5. Results

The initial lithospheric model, as previously described, was refined through a manual, iterative 2D integrated modelling approach to achieve the best possible joint fit to all input geophysical datasets. Adjustments were made to the geometry and depth of density discontinuities and lithospheric units wherever necessary, along with modifications to thermal and density-related parameters. Given that near-surface structures (such as sedimentary layers and the upper crust) are relatively well constrained, the most substantial revisions were applied to deeper features, particularly the Moho and the lithosphere–asthenosphere boundary (LAB). The modelling process continued until a satisfactory fit was reached between the observed geophysical data and the model-predicted responses. The final model is shown in Fig. 3, together with by the calibrated set of density and thermal parameters listed in Table 1.

The main focus of our study is the calculation of depth and shape of the LAB along the profile Vyhne. Beneath the European platform and Outer Western Carpathians, the LAB trend is almost flat with depths about 115–

Table 1. Densities and thermal properties of the different bodies used in integrated modelling along profile Vyhne. No: Reference number in Fig. 2, HP: heat production ( $\mu\text{Wm}^{-3}$ ), TC: thermal conductivity ( $\text{Wm}^{-1}\text{K}^{-1}$ ),  $\rho_0$ : density at room temperature ( $\text{kgm}^{-3}$ ).

Nr.	Unit	HP	TC	$\rho_0$
1	Neogene sediments 1	3.0	2.5	2450
2	Neogene sediments 2	3.0	2.5	2550
3	European platform cover	1.0	2.5	2500
4	Carpathian Foredeep	2.5	2.5	2500
5	Outer Carpathian Flysch Belt	2.0	2.5	2650
6	European platform upper crust	1.0	2.5	2750
7	Western Carpathian upper crust	2.5	3.0	2750
8	Pannonian Basin upper crust	2.5	3.0	2750
9	European platform and Western Carpathian lower crust	0.2	2.0	3000
10	Pannonian Basin lower crust	0.2	2.0	3000
11	European platform and Western Carpathian lower (mantle) lithosphere	0.05	3.4	3200 + (3325)
12	Pannonian Basin lower (mantle) lithosphere	0.05	3.4	3200 + (3325)

118 km. Towards the Inner Western Carpathians, slight lithospheric thickening can be observed, as well as a formation of a weakly pronounced lithospheric root which can be interpreted as a small remnant of a subducted slab. This lithospheric root was described by *Spakman et al. (1993)*, *Lillie et al. (1994)*, and *Wortel and Spakman (2000)* and it has also been detected in the previous work of *Zeyen et al. (2002)* and *Dérerová et al. (2006)*. The depth of LAB at the location of Vyhne tidal station is 113 km. In the Pannonian Basin, the modelled depth rapidly decreases to 80 km.

The Moho beneath the European platform reaches values up to 35 km. In the Western Carpathians, we observe slight thickening of Moho up to 37 km. These values are in correlation with our previous modelling (*Zeyen et al., 2002*) and *Bielik et al. (2018)*. The Moho depth at the location of Vyhne tidal station is 31.4 km. The Moho boundary beneath the Pannonian Basin shows a stable trend of approximately 25 km.

The depth of the boundary between upper and lower crust changes minimally and varies between 17 and 19 km, which is in correlation with data

published by *Bielik (1995)*. Under the European platform and the Western Carpathians, the trend varies from 17 to 20 km, while in the Pannonian Basin, the values are almost constant (on average it is about of 18 km).

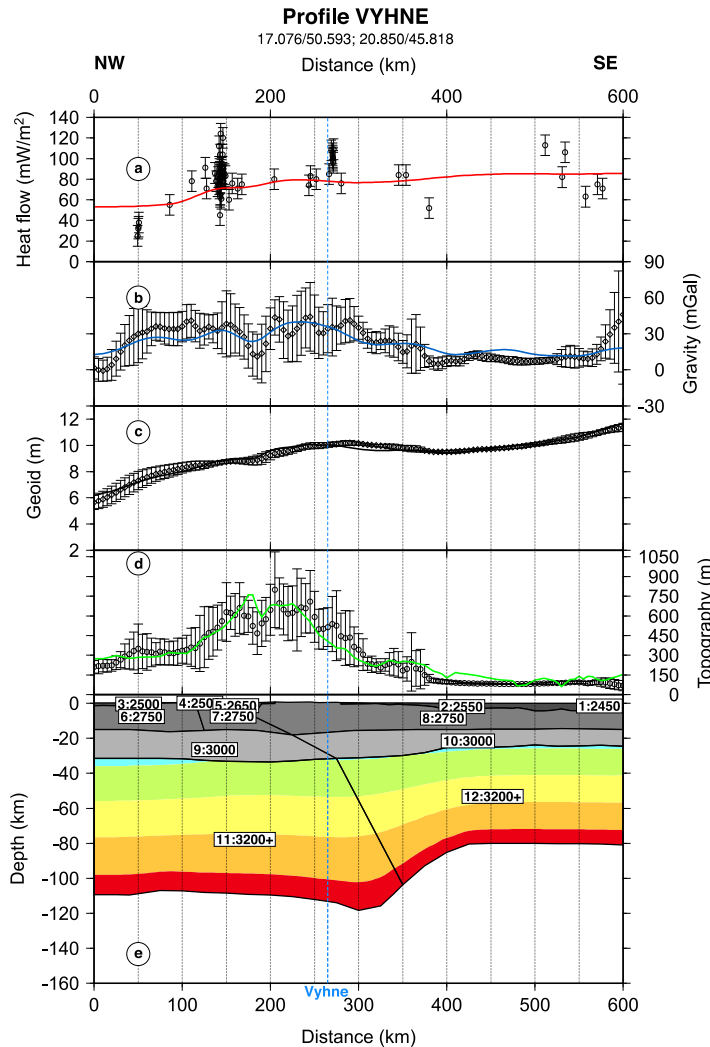


Fig. 3. Lithospheric model along profile Vyhne. (a) Surface heat flow, (b) free air gravity anomaly, (c) geoid, (d) topography with dots corresponding to measured data with uncertainty bars and solid lines to calculated values. Numbers in (e) correspond to material number in Table 1.

The sedimentary layer changed minimally and it's in agreement with data published by and *Makarenko et al. (2002)*. In our modelling, the densities of sediments are constant; we don't consider lateral or with-depth variations because it has negligible effect on our calculations.

In order to fit the surface heat flow data, the upper and lower crust had to be divided into two units that differ in their thermal parameters, while the densities remain the same.

We have calculated temperature distribution for a given lithospheric structure along profile Vyhne (Fig. 4), where the lower limit of the model corresponds to 1300 °C isotherm. The resulting temperature field is determined by the effect of the heat sources and background heat flow density from the lower mantle. The Moho temperature at the location of Vyhne tidal station is 599 °C.

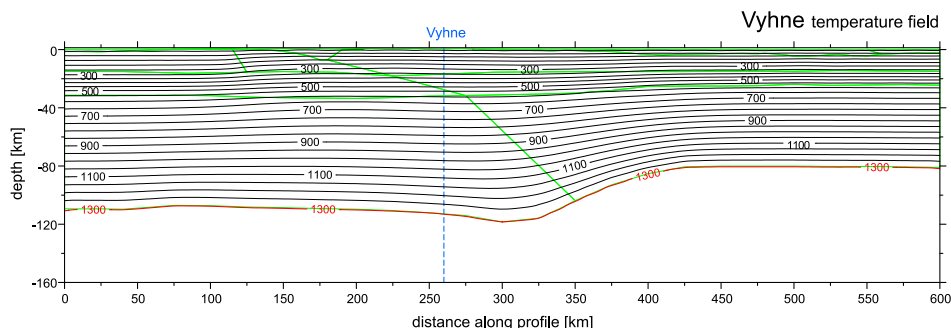


Fig. 4. Lithospheric temperature distribution calculated for profile Vyhne, isolines every 200 °C. The bottom of the model corresponds to the 1300 °C isotherm (red line). Green lines show contours of individual bodies comprising the lithospheric model.

Based on the calculated temperature distribution and given rheological parameters (Tables 2a and 2b) we have calculated the brittle and ductile strength distribution in the lithosphere. The minimum of these two values represents the yield strength, for both compressional and extensional regimes (Figs. 5 and 6). In our calculations we adopted the strain rate value of  $10^{-15} \text{ s}^{-1}$ .

The results of yield strength contour plot for both compressional and extensional deformation show that the largest strength occurs on the boundary between the upper and lower crust. Compressional regime is dominant, with the highest values of strength beneath the European platform and the Western Carpathians.

Table 2a. General properties used for producing the rheological model along the profile Vyhne.

Definition	Parameter	Value
Gravity acceleration [ $\text{ms}^{-2}$ ]	$g$	9.81
Universal gas constant [ $\text{J mol K}^{-1}$ ]	$R$	8.314
Temperature at the base of the lithosphere [ $^{\circ}\text{C}$ ]	$T_m$	1300
Static friction coefficient	$f_s$	0.7
Strain rate [ $\text{s}^{-1}$ ]	$\dot{\varepsilon}$	$10^{-15}$
Hydrostatic pore fluid factor	$\lambda$	0.4

Table 2b. Thermal and rheological parameters used for modelling along profile Vyhne (after *Carter and Tsenn (1987)*; *Goetze and Evans (1979)* and *Lankreijer et al., (1999)*). HP: heat production ( $\mu\text{W m}^{-3}$ ), TC: thermal conductivity ( $\text{W m}^{-1} \text{K}^{-1}$ ),  $\rho_0$ : density at room temperature ( $\text{kg m}^{-3}$ ),  $A_p$ : power law pre-exponential constant,  $n$ : power law exponent,  $E_p$ : power law activation energy ( $\text{kJ mol}^{-1}$ ).

Nr.	Unit	HP	TC	$\rho_0$	$A_p$	$n$	$E_p$
1	Neogene sediments 1	3.0	2.5	2450	3.16E-26	3.30	186.5
2	Neogene sediments 2	3.0	2.5	2550	3.16E-26	3.30	186.5
3	European platform cover	1.0	2.5	2500	3.16E-26	3.30	186.5
4	Carpathian Foredeep	2.5	2.5	2500	3.16E-26	3.30	186.5
5	Outer Carpathian Flysch Belt	2.0	2.5	2650	3.16E-26	3.30	186.5
6	European platform upper crust	1.0	2.5	2750	3.16E-26	3.30	186.5
7	Western Carpathian upper crust	2.5	3.0	2750	3.16E-26	3.30	186.5
8	Pannonian Basin upper crust	2.5	3.0	2750	3.16E-26	3.30	186.5
9	European platform and Western Carpathian lower crust	0.2	2.0	3000	6.31E-20	3.05	276.0
10	Pannonian Basin lower crust	0.2	2.0	3000	6.31E-20	3.05	276.0
11	European platform and Western Carpathian lower (mantle) lithosphere	0.05	3.4	3200+ (3325)	7.94E-18	4.50	535.0
12	Pannonian Basin lower (mantle) lithosphere	0.05	3.4	3200+ (3325)	7.94E-18	4.50	535.0

The strength distribution, when integrated along vertical lithospheric columns, allows to compare the resistance of the lithosphere to stress in different areas. Figure 7 shows that the highest strength (compressional)

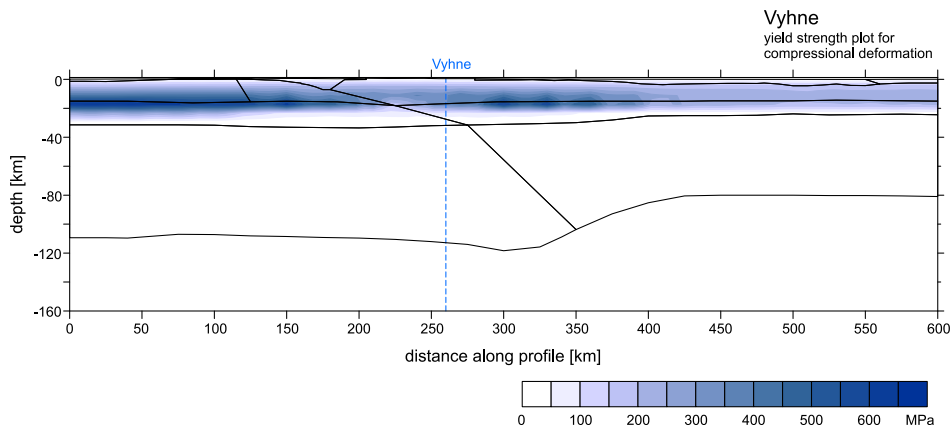


Fig. 5. Yield strength contour plot for compressional deformation calculated along profile Vyhne respective to a strain rate  $10^{-15} \text{ s}^{-1}$ .

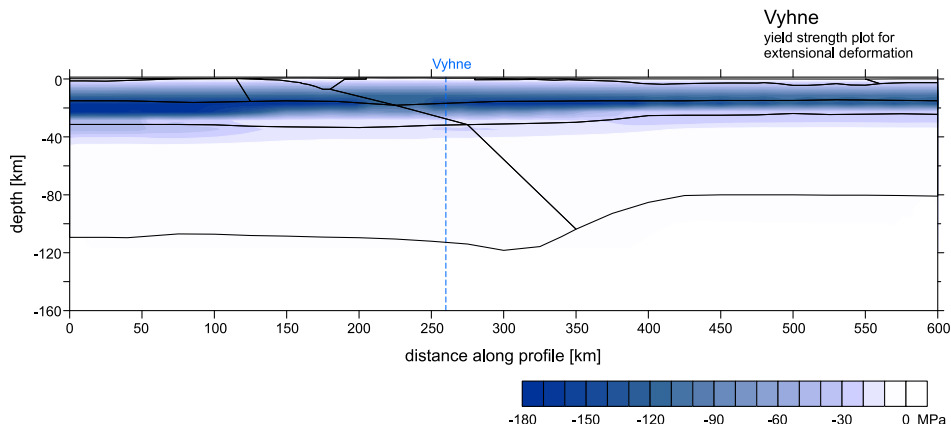


Fig. 6. Yield strength contour plot for extensional deformation calculated along profile Vyhne respective to a strain rate  $10^{-15} \text{ s}^{-1}$ .

occurs beneath the European platform and the Western Carpathians. Following the calculated line, the strength decreases from its high values in the European platform towards its minimum in Pieniny Klippen Belt. Then, it increases again, reaching maximum values in the Western Carpathians. As the profile continues towards the Pannonian Basin, the strength rapidly decreases and reaches its flat minimum.

We have calculated the strength distribution and constructed the yield strength envelope for lithospheric column that corresponds to location of

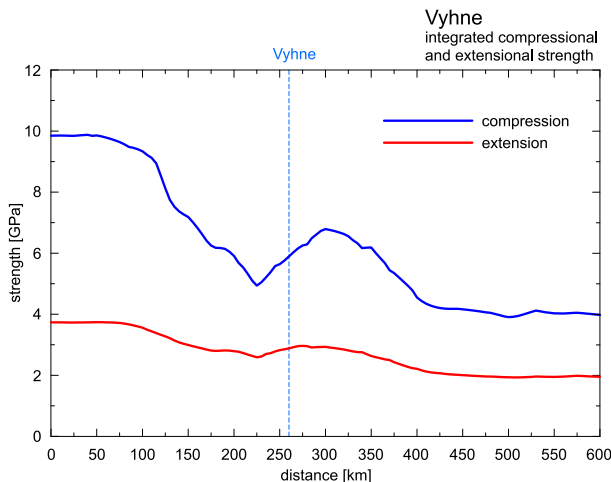


Fig. 7. Vertically integrated compressional (blue line) and extensional (red line) strength calculated along profile Vyhne.

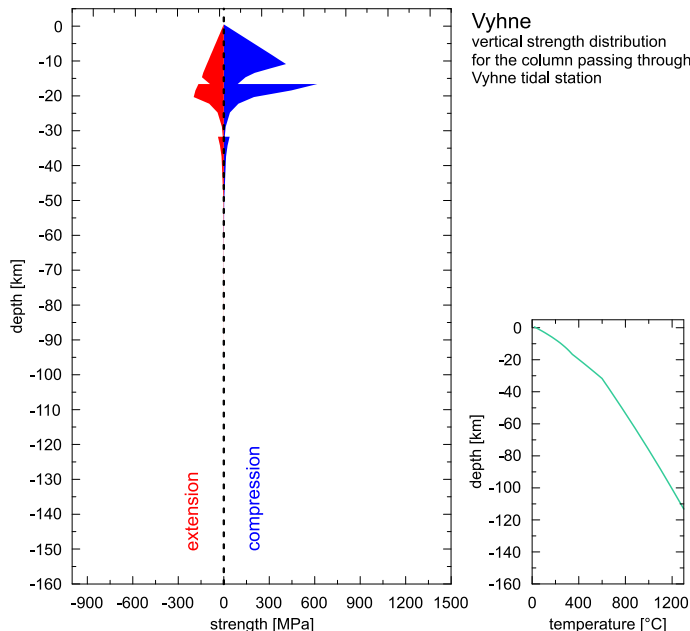


Fig. 8. Vertical strength distribution for lithospheric column corresponding to the location of Vyhne tidal station on profile Vyhne. Negative and positive values correspond to extensional and compressional strength, respectively.

Vyhne tidal station (Fig. 8). The yield strength envelope is represented by the curves of two different types. At shallow depths, the straight line corresponding to brittle failure shows the increase of strength with depth. At greater depths the curved line, corresponding to ductile deformation, shows the decrease of strength with depth due to temperature increase.

## 6. Conclusions

We constructed deep lithospheric structure model based on 2D integrated modelling. Several geophysical datasets have been used (surface heat flow measurements, topography, gravity anomalies, and short-wavelength geoid height data), together with available geological information. The resulting model shows clearly that beneath the European Platform and the Outer Western Carpathians, the LAB is nearly horizontal, lying at depths of approximately 115–118 km. Moving toward the Inner Western Carpathians, a modest increase in lithospheric thickness becomes apparent, along with the presence of a subtly developed lithospheric root, which may represent a small remnant of the upper part of the break-off subducted lithospheric slab. The contact zone between the Inner Western Carpathians and the Pannonian Basin is represented by a sharp change in LAB depth (from 110 to 80 km). The lithospheric thickness in the Pannonian Basin is about 80 km. The Moho boundary beneath the European platform reaches values up to 35 km. In the Western Carpathians, we observe slight thickening of Moho up to 37 km. The Moho boundary beneath the Pannonian Basin shows a stable trend of approximately 25 km.

Our rheological results show that the compressional regime is dominating and the highest strength occurs beneath the European platform and the Western Carpathians. Following the calculated line, the strength decreases from its high values in the European platform towards its minimum in the Pieniny Klippen Belt. Then, it increases again, reaching maximum values in the Western Carpathians. The calculated model of the lithosphere along profile Vyhne will provide additional information to serve for tectonic interpretation and geodynamical reconstruction of the area where the tidal station Vyhne is located.

**Acknowledgements.** This research was supported by the Slovak Research and Development Agency under the contracts No. APVV-21-0159, APVV-24-0445, and the

VEGA Slovak Grant Agency under project No. 2/0013/25. Authors are grateful to Prof. Hermann Zeyen of University de la Terre for permission to use 2D integrated modelling software. The work was carried out within the framework of bilateral scientific co-operation between the National Academy of Sciences of Ukraine and the Slovak Academy of Sciences.

## References

Bielik M., 1995: Continental convergence in the area of the Western Carpathians on the basis of density modeling. *Geol. Carpath.*, **46**, 1, 3–12.

Bielik M., Alasonati-Tašárová Z., Zeyen H., Dérerová J., Afonso J. C., Csicsay K., 2010: Improved geophysical image of the Carpathian-Pannonian Basin region. *Acta Geod. Geophys. Hung.*, **45**, 3, 284–298, doi: [10.1556/AGeod.45.2010.3.3](https://doi.org/10.1556/AGeod.45.2010.3.3).

Bielik M., Makarenko I., Csicsay K., Legostaeva O., Starostenko V., Savchenko A., Šimonová B., Dérerová J., Fojtíková L., Paštka R., Vozár J., 2018: The refined Moho depth map in the Carpathian-Pannonian region. *Contrib. Geophys. Geod.*, **48**, 2, 179–190, doi: [10.2478/congeo-2018-0007](https://doi.org/10.2478/congeo-2018-0007).

Brimich L., 1988: Extensometric measurements at the Vyhne tidal station. *Contrib. Geophys. Inst. Slov. Acad. Sci.*, **18**, 58–62.

Brimich L., Bednárik M., Bezák V., Kohút I., Bán D., Eperne-Pápai I., Mentes G., 2016: Extensometric observation of Earth tides and local tectonic processes at the Vyhne station, Slovakia. *Contrib. Geophys. Geod.*, **46**, 2, 75–90, doi: [10.1515/congeo-2016-0006](https://doi.org/10.1515/congeo-2016-0006).

Byerlee J., 1978: Friction of rocks. *Pure Appl. Geophys.*, **116**, 4–5, 615–626, doi: [10.1007/BF00876528](https://doi.org/10.1007/BF00876528).

Carter N. L., Tsenn M. C., 1987: Flow properties of continental lithosphere. *Tectonophysics*, **136**, 1-2, 27–63, doi: [10.1016/0040-1951\(87\)90333-7](https://doi.org/10.1016/0040-1951(87)90333-7).

Csontos L., Vörös A., 2004: Mesozoic plate tectonic reconstruction of the Carpathian region. *Palaeogeogr. Palaeoclimatol. Palaeoecol.*, **210**, 1, 1–56, doi: [10.1016/j.palaeo.2004.02.033](https://doi.org/10.1016/j.palaeo.2004.02.033).

Dadlez R., Grad M., Guterch A., 2005: Crustal structure below the Polish Basin: is it composed of proximal terranes derived from Baltica? *Tectonophysics*, **411**, 1–4, 111–128, doi: [10.1016/j.tecto.2005.09.004](https://doi.org/10.1016/j.tecto.2005.09.004).

Dérerová J., Zeyen H., Bielik M., Salman K., 2006: Application of integrated geophysical modelling for determination of the lithospheric structure in the Western Carpathians. *Tectonics*, **25**, 3, TC3009, doi: [10.1029/2005TC001883](https://doi.org/10.1029/2005TC001883).

Dudášová V., 1998: Description of the renovated extensometer at the Vyhne tidal station. *Contrib. Geophys. Geod.*, **28**, 3, 197–203.

Froitzheim N., Plašienka D., Schuster R., 2008: Alpine tectonics of the Alps and Western Carpathians. In: McCann T. (Ed.): *The Geology of Central Europe Volume 2: Mesozoic and Cenozoic*. Geological Society, London, pp. 1141–1232, doi: [10.1144/CEV2P.6](https://doi.org/10.1144/CEV2P.6).

Gesch D. B., Verdin K. L., Greenlee S. K., 1999: New land surface digital elevation model covers the Earth. *Eos Trans. AGU*, **80**, 6, 69–70, doi: [10.1029/99EO000050](https://doi.org/10.1029/99EO000050).

Goetze C., Evans B., 1979: Stress and temperature in the bending lithosphere as constrained by experimental rocks mechanics. *Geophys. J. R. Astron. Soc.*, **59**, 3, 463–478, doi: 10.1111/j.1365-246X.1979.tb02567.x.

Golonka J., Oszczypko N., Ślaczka A., 2000: Geodynamic evolution and paleogeography of the Carpathian–Pannonian region – a global perspective. *Slovak Geol. Mag.*, **6**, 2–3, 139–142.

Hók J., Bielik M., Kováč P., Šujan M., 2000: Neotektonický charakter územia Slovenska (Neotectonic character of Slovakia). *Miner. Slovaca*, **32**, 5, 459–470 (in Slovak, English summary).

Kilényi E., Šefara J. (Eds.), 1989: Pre-Tertiary basement contour map of the Carpathian Basin beneath Austria, Czechoslovakia and Hungary. ELGI, Budapest.

Konečný V., Lexa J., Šimon L. Dublan L., 2001: Neogénny vulkanizmus stredného Slovenska (The neogene volcanism in central Slovakia). *Miner. Slovaca*, **33**, 3, 159–178 (in Slovak, English summary).

Kováč M., 2000: Geodynamický, paleografický a štruktúrny vývoj Karpatsko-Panónskeho regiónu v Miocene: Nový pohľad na neogénne panvy Slovenska (Geodynamic, palaeogeographic and structural evolution of the Carpathian-Pannonian region during Miocene: New view on the Neogene basins in Slovakia). VEDA, Bratislava, 202 p. (in Slovak with English summary).

Kováč M., Kráľ J., Márton E., Plašienka D., Uher P., 1994: Alpine uplift history of the Central Western Carpathians: geochronological, paleomagnetic, sedimentary and structural data. *Geol. Carpath.*, **45**, 2, 83–96.

Kováč M., Márton E., Oszczypko N., Vojtko R., Hók J., Králiková S., Plašienka D., Klučiar T., Hudáčková N., Oszczypko-Clowes M., 2017: Neogene palaeogeography and basin evolution of the Western Carpathians, Northern Pannonian domain and adjoining areas. *Glob. Planet. Change*, **155**, 133–154, doi: 10.1016/j.gloplacha.2017.07.004.

Krejčí O., Jurová Z., 1997: Strukturní mapa báze sedimentu flyšových příkrovů s vyznačením prognózních ploch (Structural map of the flysch sediment base with marked forecast areas). Manuskript ČGÚ Brno (in Czech).

Lachenbruch A. H., Morgan P., 1990: Continental extension, magmatism and elevation; formal relations and rules of thumb. *Tectonophysics*, **174**, 1–2, 39–62, doi: 10.1016/0040-1951(90)90383-J.

Lankreijer A., Bielik M., Cloetingh S., Majcen D., 1999: Rheology predictions across the western Carpathians, Bohemian Massif, and the Pannonian Basin: Implications for tectonic scenarios. *Tectonics*, **18**, 6, 1139–1153, doi: 10.1029/1999TC900023.

Lexa J., Konečný V., 1998: Geodynamic aspects of the Neogene to Quaternary volcanism. In: Rakús M. (Ed.): *Geodynamic Development of the Western Carpathians. Geological Survey of Slovak Republic*, Bratislava, pp. 219–240.

Lexa J., Štohl J., Konečný V., 1999: The Banská Štiavnica ore district: relationship between metallogenetic processes and the geological evolution of a stratovolcano. *Miner. Depos.*, **34**, 5–6, 639–654, doi: 10.1007/s001260050225.

Lexa J., Seghedi I., Németh K., Szakács A., Konečný V., Pécsay Z., Fülöp A., Kovacs M., 2010: Neogene-Quaternary Volcanic forms in the Carpathian-Pannonian Region: a review. *Cent. Eur. J. Geosci.*, **2**, 3, 207–270, doi: 10.2478/v10085-010-0024-5.

Lillie J. R., Bielik M., Babuška V., Plomerová J., 1994: Gravity modelling of the lithosphere in the Eastern Alpine–Western Carpathian–Pannonian Basin Region. *Tectonophysics*, **231**, 4, 215–235, doi: 10.1016/0040-1951(94)90036-1.

Lynch H. D., Morgan P., 1987: The tensile strength of the lithosphere and the localization of extension. In: Coward M. P., Dewey J. F., Hancock P. L. (Eds.): *Continental Extensional Tectonics*. *Geol. Soc. Spec. Publ.*, **28**, pp. 53–65, doi: 10.1144/GSL.SP.1987.028.01.05.

Makarenko I., Legostaeva O., Bielik M., Starostenko V., Dérerová J., Šefara J., 2002: 3D gravity effects of the sedimentary complexes in the Carpathian-Pannonian region. *Geologica Carpathica*, **53**, special issue, Proc. XVII. Congress of Carpathian-Balkan Geological Association, Bratislava, September 1-4, 2002.

Mazur S., Krzywiec P., Malinowski M., Lewandowski M., Aleksandrowski P., Mikołajczak M., 2018: On the nature of the Teisseyre-Tornquist Zone. *Geol. Geophys. Environ.*, **44**, 1, 17–30, doi: 10.7494/geol.2018.44.1.17.

Pavlis N. K., Holmes S. A., Kenyon S. C., Factor J. K., 2008: An Earth gravitational model to degree 2160: EGM2008. General Assembly of the European Geosciences Union, Vienna, Austria, April 13–18, 2008, *Geophysical Research Abstracts*, Vol. 10, EGU2008-A-01891.

Pharaoh T. C., 1999: Palaeozoic terranes and their lithospheric boundaries within the Trans-European Suture Zone (TESZ): A review. *Tectonophysics*, **314**, 1–3, 17–41, doi: 10.1016/S0040-1951(99)00235-8.

Plašienka D., 2003: Development of basement-involved fold and thrust structures exemplified by the Tatic–Fatic–Veporic system of the Western Carpathians (Slovakia). *Geodin. Acta*, **16**, 1, 21–38, doi: 10.1016/S0985-3111(02)00003-7.

Plašienka D., Grecula P., Putiš M., Kováč M., Hovorka D., 1997: Evolution and structure of the Western Carpathians: An overview. In: Grecula P., Hovorka D., Putiš M. (Eds.): *Geological evolution of the Western Carpathians*. Miner. Slovaca, Monograph, pp. 1–24.

Pollack H. N., Hurter S. J., Johnson J. R., 1993: Heat flow from the Earth's interior: Analysis of the global data set. *Rev. Geophys.*, **31**, 3, 267–280, doi: 10.1029/93RG01249.

Ranalli G., 1995: *Rheology of the Earth*. 2nd ed., Springer, 414 p.

Royden L. H., Horváth F., 1988: The Pannonian Basin: A study in basin evolution. *AAPG Mem.*, **45**, 0065-731X, 394 p.

Sandwell D. T., Smith W. H. F., 1997: Marine gravity anomalies from Geosat and ERS-1 satellite altimetry. *J. Geophys. Res. Solid Earth*, **102**, B5, 10039–10054, doi: 10.1029/96JB03223.

Schmid S. M., Bernoulli D., Fügenschuh B., Matenco L., Schefer S., Schuster R., Tischler M., Ustaszewski K., 2008: The Alpine–Carpathian–Dinaridic orogenic system: Correlation and evolution of tectonic units. *Swiss J. Geosci.*, **101**, 1, 139–183, doi: 10.1007/s00015-008-1247-3.

Spakman W., van der Lee S., van der Hilst R., 1993: Travel-time tomography of the European–Mediterranean mantle down to 1400 km. *Phys. Earth Planet. Inter.*, **79**, 1–2, 3–74, doi: 10.1016/0031-9201(93)90142-V.

Talwani M., Worzel J. L., Landisman M., 1959: Rapid gravity computations for two-dimensional bodies with application to the Mendocino submarine fracture zone. *J. Geophys. Res.*, **64**, 1, 49–59, doi: 10.1029/JZ064i001p00049.

Tomek Č., Hall J., 1993: Subducted continental margin imaged in the Carpathians of Czechoslovakia. *Geology*, **21**, 6, 535–538, doi: 10.1130/0091-7613(1993)021<0535:SCMIIN>2.3.CO;2.

Wortel M. J. R., Spakman W., 2000: Subduction and slab detachment in the Mediterranean–Carpathian region. *Science*, **290**, 5498, 1910–1917, doi: 10.1126/science.290.5498.1910.

Zeyen H., Fernández M., 1994: Integrated lithospheric modeling combining thermal, gravity, and local isostasy analysis: Application to the NE Spanish Geotransect. *J. Geophys. Res. Solid Earth*, **99**, B9, 18089–18102, doi: 10.1029/94JB00898.

Zeyen H., Dérerová J., Bielik M., 2002: Determination of the continental lithospheric thermal structure in the Western Carpathians: Integrated modelling of surface heat flow, gravity anomalies and topography. *Phys. Earth Planet. Inter.*, **134**, 1–2, 89–104, doi: 10.1016/S0031-9201(02)00155-3.

Zeyen H., Ayarza P., Fernández M., Rimi A., 2005: Lithospheric structure under the western African–European plate boundary: A transect across the Atlas Mountains and the Gulf of Cadiz. *Tectonics*, **24**, 2, TC2001, doi: 10.1029/2004TC001639.

Ziegler P. A., 1990: Geological Atlas of Western and Central Europe. 2nd Edition, Shell Internationale Petroleum Maatschappij BV, Geological Society, London, 239 p.